https://doi.org/10.22226/2410-3535-2023-2-171-176



# Elastic properties of diamane

P. V. Polyakova[1], L. Kh. Galiakhmetova[†,1], R. T. Murzaev[1],
D. S. Lisovenko[2], J. A. Baimova[1]

[†]rysaeva.l.h@gmail.com

[1]Institute for Metals Superplasticity Problems, RAS, Ufa, 450001, Russia
[2]Ishlinsky Institute for Problems in Mechanics, RAS, Moscow, 119526, Russia

Diamane is a two-dimensional carbon-based structure coated with hydrogen atoms. The stiffness constants of diamane are studied by molecular dynamics simulation. These constants are used for an analytical calculation of Young's modulus, Poisson's ratio, and shear modulus. Two different morphologies are considered, namely, AA diamane and AB diamane. Moreover, both morphologies can contain hydrogen or be without it. It is found that pristine diamane without hydrogen demonstrates higher stiffness constants due to the changes in hybridization. At the same time, the difference in the values of the constants for the two diamane morphologies AA and AB is insignificant. All the obtained results are compared with elastic constants of graphene and diamond calculated by the same method and obtained from literature. Young's modulus of pristine diamane equal to 1182 GPa is close to that of for graphene diamond.

**Keywords:** diamane, elastic constants, molecular dynamics, mechanical properties.

## 1. Introduction

The novel two-dimensional (2D) structures are the thinnest functional materials having macroscopic planar lengths and atomically thin. Such 2D materials have distinctive physical and mechanical characteristics and chemical reactivity [1]. The relationship between their structure and properties is of great interest because of their unusual atomic structures. These 2D materials are crucial for different kinds of utilizations, such as catalysts, optoelectronics, spintronics, biological and chemical sensors, photovoltaic, lithium-ion batteries, and supercapacitors [2]. This constantly growing interest started in 2004 after the mechanical exfoliation of graphene — a monoatomic layer of graphite [3]. A considerable number of new physical effects were discovered for this material, which arises from its 2D nature. Graphene has high mechanical rigidity and high thermal conductivity, and the record carrier mobility makes it a promising material for a wide variety of applications, in particular, for future electronics [4–6]. In addition to graphene, there is a huge family of other new 2D structures. Understanding the fundamental properties of 2D structures is important for the development of low-dimensional physics and chemistry.

One such 2D structure is diamane, which was theoretically proposed in [7]. Diamane is composed of two graphene layers connected by a covalent bond and covered with hydrogen atoms. Diamane is a two-dimensional diamond-like structure and can be defined as $C_2H$. Diamane is the thinnest diamond film and can demonstrate all the unique mechanical properties of diamond films [8]. Different properties of diamane were studied by computer simulation and it was shown that diamane can be used in nano-photonics and ultrasensitive resonator-based sensors [9–12]. Recently, the fully fluorinated AB-stacked diamane and pristine diamane were successfully synthesized experimentally [13]. It should be noted that different names, such as diamane, diamondol, diamondene, or diamene were adopted for diamane, due to the diversity of surface functional groups on the diamond film surface. Here, the term "diamane", which was introduced by Chernozatonskii et al. [7] is used. Diamane can be doped not only with hydrogen but also with fluorine and chlorine. The properties of such structures were studied in [14].

Significant progress has been made in obtaining and studying diamane by experimental methods, as indicated in the recent review [15]. For the first time in [16], the synthesis of stable nanometer-sized crystalline $sp^3$-bound carbon was shown. Diamane was obtained by chemisorption of H-radicals formed during the hot filament process at low temperature and pressure. At the moment, diamanes are observed mainly in the Raman spectra [16]. According to calculations, diamane is a semiconductor material with a direct wide band gap, which is very attractive for nanoelectronics [17,18]. Due to the supposed high thermal conductivity, diamane can be used in temperature control devices [19]. Diamane is also expected to be very rigid, which is very attractive for ultra-thin protective coatings, ultra-high-strength components in composite materials for aerospace applications, for example, and nanoelectromechanical systems [19]. Due to the expected low friction coefficient of a hydrogenated surface, diamane can also be used to increase the wear resistance of coated mechanical parts.

There are a large number of theoretical and experimental methods for studying two-dimensional structures. Theoretical studies make it possible to choose the conditions for further experimental studies. For example, optical spectra, and tensile strength were studied by density functional theory (DFT)

for diamane [14, 20 – 22]. In [23 – 25] interatomic potentials to study 2D carbons are discussed. Methods for calculating elastic constants are described using a discrete model. However, molecular dynamics (MD) also can be effectively used for the study of the physical and mechanical properties of diamane. For example, the mechanical properties of diamane under tensile and bending deformation were studied in [26]. It was shown that layer stacking has almost no effect on the mechanical strength of diamane, and similar Young's modulus are found along the zigzag and armchair directions. The diamane fracture is dominated by the crack propagation along zigzag directions, which is independent of the tensile directions. The mechanical behavior of interlayer-bonded nanostructures obtained from bilayer graphene was also studied in [27].

Although extensive works have been done to date on the study of the mechanical properties of diamane, there is a lack of understanding of the relationship between mechanical properties and structure, especially in the elastic regime. In this work, stable two-dimensional structures of AA and AB pure and hydrogenated diamane are studied by molecular dynamics. Stiffness constants are calculated from MD simulation and used for analytical calculations of Young's modulus, shear modulus, and Poisson's ratio.

## 2. Simulation details

### 2.1. Initial structure

In Fig. 1a, the simulation cell for the calculation of elastic constants of diamane is shown. The insets in the circles show the structure in two projections *xy* and *xz*, where the orange atoms represent hydrogen and the gray ones represent carbon. The thickness of diamane is *h* and the sizes of the simulation cell are *a*, *b*, and *c* along *x*, *y*, and *z* directions.

Diamane has two stable configurations [7,17,18]: AA is composed of graphene layers located one above the other, and hydrogen atoms are arranged in a checkerboard pattern; and AB is a Bernal-stacked form of bilayer graphene. Both structures have a hexagonal symmetry. For convenience, further diamonds will be abbreviated as D-AA and D-AB. Moreover, since structures with and without hydrogen are considered, the abbreviations D-AA+H and D-AB+H will be further used.

The periodic cells of diamanes are presented in Fig. 1b, c. For both D-AA and D-AB, the periodic cell consists of four carbon atoms (colored gray) and two hydrogen atoms (colored orange). Each carbon atom has $sp^3$-hybridization.

The thickness of diamane is equal to 6.8 Å for structures with hydrogen and 4.6 Å without hydrogen [22, 26]. Two sizes of the diamane are considered: 250 × 250 Å and 1000 ×1000 Å. Thus, $a = b = 250; 1000$ Å. The boundary conditions are periodic along all directions. However, to neglect the interaction between diamane in the periodic cells, the size of the simulation cell along *z*-axis is taken much larger than the diamane thickness ($c = 20$ Å). Three lengths of the simulation cell normal to diamane plane ($c$) are considered initially: 20, 50, and 100 Å. It was found, that the increase of the length of the simulation cell above 20 Å does not affect the values of strain that appeared in the structure during deformation. The same length of the simulated cell was also used previously in the literature [14, 28].

Table 1 lists the main structural characteristics of diamanes, such as the number of atoms in a unit cell ($N_{at}$),

**Table 1.** Structural characteristics of diamane: $N_{at}$ is the number of atoms in a unit cell, $l_i$ ($i$ =1, 4) is the bond length, $a_x$ and $a_y$ are the translation parameters.

| Structure | $N_{at}$ | $l_1$ (C-H), Å | $l_2$, Å | $l_3 = l_4$, Å | angle α,° | $a_x$, Å | $a_y$, Å |
|---|---|---|---|---|---|---|---|
| D-AA+H | 6 | 1.10 | 1.52 | 1.53 | 107.9 | 2.189 | 2.194 |
| D-AB+H | 6 | 1.12 | 1.58 | 1.51 | 107.7 | 1.263 | 1.266 |

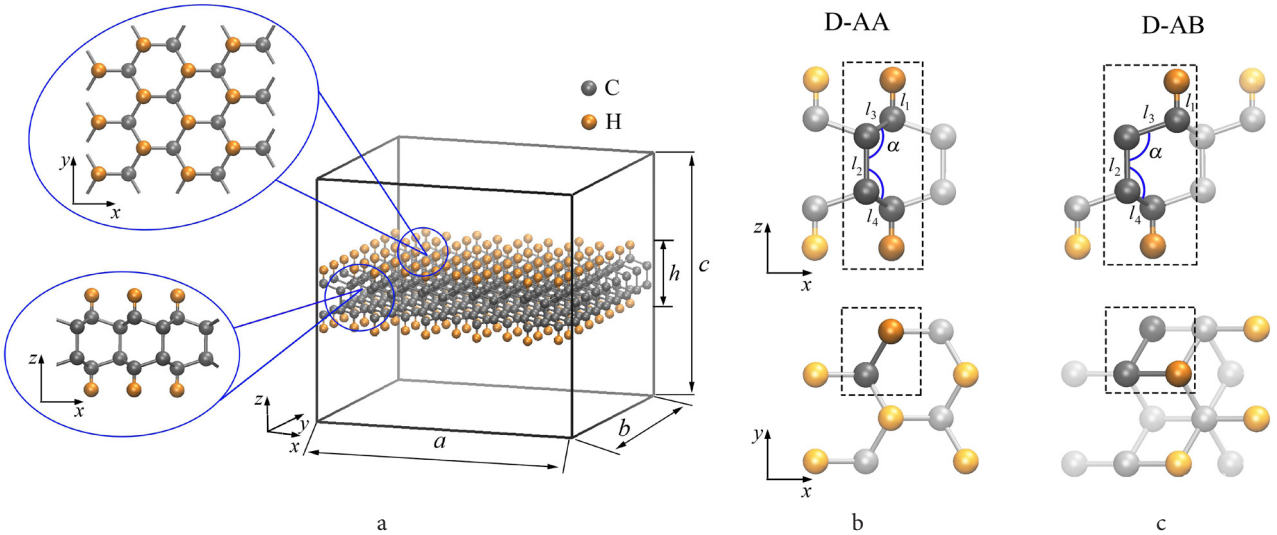


**Fig. 1.** (Color online) The simulation cell used for the calculation of elastic constants of diamane. The insets show projections on the *xy* and *xz* planes. Carbon atoms are colored gray, and hydrogen atoms are colored orange (a). Periodic cells of diamanes D-AA and D-AB in two projections (b, c). The bond lengths are defined as $l_i$, and valent angles — as α. The unit cell is indicated by dotted lines.

bond lengths ($l_i$), principal angle (α), and translation parameters for the periodic cell ($a_x$, $a_y$). The bond lengths and angles are presented in Fig. 1b, c. The structural parameters considered in this work are in good agreement with the ones calculated by the DFT [7]. According to the structural characteristics, the angles in the cell have the same value and are close to the angle between the atoms in a diamond, the bond lengths $l_2$ and $l_3 = l_4$.

All calculations were performed using the LAMMPS [29–31] software package with the AIREBO interatomic potential [32], which has been successfully used to study various properties of a large number of carbon nanosystems including diamane [33–36]. The cutoff distance in the switching function of AIREBO potential is set as 2.0 Å to avoid spurious high stress at higher strains [27, 37]. All calculations are carried out at 0 K, so that the effect of temperature on the elastic constants can be neglected. Temperature control is carried out using a Nose-Hoover thermostat.

### *2.2. Elastic constants for two-dimensional structure*

After the equilibrium state of the structures is reached, the stiffness coefficients $c_{ij}$ are calculated. Diamane can be elastically strained up to 1–1.5%. According to Hooke's law, at small strains, the stress components σij are directly proportional to the strain components $\varepsilon_{kl}$ and have the form:

$$\sigma_{ij} = c_{ijkl} \times \varepsilon_{kl},$$

where $c_{ijkl}$ is the fourth-order tensor of stiffness constant. In this case, Hooke's law for materials with hexagonal anisotropy is written in the matrix form as follows:

$$\begin{bmatrix} \sigma_{xx} \\ \sigma_{yy} \\ \sigma_{zz} \\ \sigma_{yz} \\ \sigma_{xz} \\ \sigma_{xy} \end{bmatrix} = \begin{bmatrix} c_{11} & c_{12} & c_{13} & \cdot & \cdot & \cdot \\ c_{12} & c_{11} & c_{13} & \cdot & \cdot & \cdot \\ c_{13} & c_{13} & c_{11} & \cdot & \cdot & \cdot \\ \cdot & \cdot & \cdot & c_{44} & \cdot & \cdot \\ \cdot & \cdot & \cdot & \cdot & c_{44} & \cdot \\ \cdot & \cdot & \cdot & \cdot & \cdot & c_{66} \end{bmatrix} \begin{bmatrix} \varepsilon_{xx} \\ \varepsilon_{yy} \\ \varepsilon_{zz} \\ \varepsilon_{yz} \\ \varepsilon_{xz} \\ \varepsilon_{xy} \end{bmatrix}.$$

Here, $c_{ij}$ are the elements of stiffness constants matrix. For a hexagonal diamane, the number of independent stiffness constants is equal to five: $c_{11}$, $c_{12}$, $c_{13}$, $c_{33}$, $c_{44}$, with an additional relationship $c_{66} = 0.5(c_{11} - c_{12})$. Based on Hooke's law, the stiffness coefficients are calculated as follows:

$$c_{11} = \frac{\sigma_{xx}}{\varepsilon_{xx}}, \; c_{12} = \frac{\sigma_{yy}}{\varepsilon_{xx}}, \; c_{13} = \frac{\sigma_{zz}}{\varepsilon_{xx}},$$

$$c_{33} = \frac{\sigma_{zz}}{\varepsilon_{zz}}, \; c_{44} = \frac{\sigma_{xy}}{\varepsilon_{xy}}, \; c_{66} = \frac{\sigma_{xz}}{\varepsilon_{xz}}.$$

For hexagonal crystals, the criteria of thermal stability (Born equations) should be satisfied [38]:

$$c_{11} > |c_{12}|, \; 2c_{13}^2 < c_{33}(c_{11} + c_{12}), \; c_{33} > 0, \; c_{44} > 0.$$

The above equations are usually applied to a three-dimensional crystal, but diamane is two-dimensional one and the thickness along *z*-axis is very small. Thus, the number of stiffness coefficients $c_{ij}$ is reduced to three — $c_{11}$, $c_{12}$, $c_{66}$, and the Born criteria change accordingly:

$$c_{11} > |c_{12}|, \; c_{66} > 0.$$

To calculate the stiffness constants of diamane, a deformation is applied to the simulation cell, and the corresponding stresses are calculated. Stiffness constants are calculated from the above equations.

However, when a 2D structure with the thickness *h* is considered, which is much larger than the size of the simulation cell *c*, the stresses must be converted from the stress acting on the simulation cell $\sigma_{box}$ [26] in terms of geometrical parameters as:

$$\sigma = \frac{\sigma_{box} c}{h}.$$

Thus, all the obtained values of stresses are corrected with the coefficient *c*/*h* to exclude the effect of boundary conditions. It should be noted, that even after the relaxation of the system, it is still not at a global minimum of potential energy, which is the limitation of the MD simulation. Minor applied strain can considerably affect the obtained elastic constants, especially for such a small 2D structure. Thus, to exclude computational errors, several numerical experiments are carried out: (1) the uniaxial tension of 0.01%, 0.05%, and 1% is applied; (2) the uniaxial compression of 0.01%, 0.05%, and 1% is applied, and (3) the undeformed structure is considered. After that, for each of these structures uniaxial tensile strain of 0.1% is applied and stiffness constants are calculated for these seven cases. Such a complicated technique is used to understand how small strains affect the resulting elastic constants. Then, from seven numerical calculations, the average values of $c_{11}$ and $c_{12}$ are found. The calculation error of not more than 4 GPa is found. Further, the average values of the stiffness constants would be presented.

The other important characteristic affecting the elastic properties of nanostructures is their size. In the present work, two sizes of the simulation cell are considered: 250×250×20 Å and 1000×1000×20 Å. It is found, that the size of the simulation cell does not affect the resulting stiffness and compliance constants for diamane: the difference between the stiffness constants is not more than 2 GPa. Thus, further only the elastic constants for the simulation cell of the smaller size are presented.

The size of the simulation cell along the thickness direction h is also taken twice as large. It is shown, that the height of the modeling cell in the *z* direction does not affect the results obtained, but should be sufficiently large compared to the thickness of the diamane.

The calculation of engineering elastic constants, such as Young's modulus *E*, shear modulus *G*, and Poisson's ratio ν is carried out analytically

$$E = c_{11} - \frac{c_{12}^2}{c_{11}}, \; G = c_{66}, \; \nu = \frac{c_{12}}{c_{11}}.$$

These formulas were derived from Hooke's law.

## 3. Results and discussion

At first, the applied methodology is used to calculate the elastic constants of the well-known materials similar to

diamane. From one point of view, it is 2D graphene, and from the other — it is 3D diamond. Graphene also has a hexagonal symmetry, and its elastic properties can be calculated from the same equations as for diamane. Stiffness coefficients, Young's modulus, and Poisson's ratio for cubic diamond were calculated in [38, 39].

Table 2 presents the compliance and stiffness coefficients obtained by MD for diamane, graphene, and diamond in the present work compared with the literature data [40, 41].

According to the data obtained (Table 2), the stiffness constants of diamane are affected by the presence of hydrogen in the structure. At the same time, the difference in the values of the constants for the two diamane morphologies AA and AB is insignificant. The stiffness constants for diamane AA and AB with H differ by 0.2 – 0.5%, and for diamane AA and AB without H constants $c_{11}$ differ by 1.5%, $c_{12}$ — 8.2%, $c_{66}$ — 6.9%.

In [39], the diamanes AA-H and AB-H are called H-diamondene, but have the same crystalline structure as in our work, so we can compare the stiffness constants with it. There is a slight difference in the constant values, which can be explained by the research methods. For graphene, stiffness constants a very close to [40], where it was obtained by asymptotic homogenization. For diamond, the proposed method gives very close values in comparison with the experimental data [41]. The difference in the experimental and theoretical values is quite reasonable: the real materials contain impurities, crystal defects, or already existing internal stresses.

The data obtained for diamane with hydrogen can also be compared with the data obtained for diamane with fluorine [28]. It was found that the stiffness constants obtained by the DFT-method are $c_{11}$ = 499.4 N/m, $c_{12}$ = 55.9 N/m. These values are also very close to the stiffness constants obtained for diamane with hydrogen.

Table 3 presents Young's modulus, Poisson's ratio and shear modulus of the diamanes under study compared to the literature date. As can be seen, the presence of hydrogen has a significant effect on the elasticity constants. The data obtained are also similar to those calculated from the DFT: 1079 GPa [43], and close to Young's modulus for graphene 1000 GPa [38], and 1050 GPa for diamond [44]. For diamane, Young's modulus does not depend on the stacking sequence, and the same along the zigzag and armchair directions. The same was shown in [26] by different simulation technique: Young's modulus was calculated from the slope of stress-strain curves.

Poisson's ratio ν for all investigated diamanes is in the range from 0.06 to 0.07, which is close to that of diamond (or diamond-like films) than for graphene (ν = 0.07, ν = 1.129, respectively) [38, 44, 50 – 53]. As can be seen, the diamane morphology has a slight effect on the stiffness constants, while the presence of hydrogen will affect elastic constants considerably. The data obtained in the present work are in good agreement with [39, 53]. It is assumed that the stiffness constants of diamanes without hydrogen are higher due to the formation of $sp^3$ bonds between carbon atoms.

**Table 2.** Stiffness $c_{ij}$ coefficients for diamane, graphene, and diamond. Stiffness constants are compared to the literature.

| Structure | $c_{11}$, GPa | $c_{12}$, GPa | $c_{66}$, GPa |
|---|---|---|---|
| Graphene | 942.7 | 340.6 | 301.9 |
| Graphene [40] | 1270.0 | 424.0 | 212.0 |
| Diamond | 1098.16 | 128.48 | 750.0 |
| Diamond [41] | 1079.0 | 124.0 | 578.0 |
| D-AA+H | 797.16 | 46.56 | 374.53 |
| D-AB+H | 798.09 | 46.03 | 375.45 |
| D-AA | 1190.0 | 62.0 | 563.7 |
| D-AB | 1187.0 | 78.51 | 549.9 |
| H-diamondene [39] | 1126.0 | 81.0 | 473.0 |

## 4. Conclusions

New two-dimensional structures — diamane of two types of morphology have been studied by molecular dynamics simulations. The stiffness constants have been calculated from molecular dynamics and then applied to calculate Young's modulus, shear modulus, and Poisson's ratio. The effect of hydrogenation on the elastic constants is also considered.

For all structural configurations, high values of stiffness constants compared to those of graphene and diamond are obtained. The data are in good agreement with the data previously obtained in the literature. The morphology of diamane has almost no effect on the elasticity constants. Increasing the size of the simulation cell also does not affect the obtained values. It is found that diamane possesses a high Young's modulus that is comparable with that of graphene, which is almost the same along the zigzag and armchair directions and independent of the stacking sequence.

The calculation methodology described in this work can be successfully applied to various two-dimensional crystals

**Table 3.** The values of Young's modulus *E*, Poisson's ratio ν, and shear modulus *G* of the diamane, graphene and diamond obtained in the present work in comparison with literature data.

| Structure | *E*, GPa | *G*, GPa | ν |
|---|---|---|---|
| Graphene | 820, 1005 [45], 725 [46], 1006 [47] | 302, 360 [48], 230 [49] | 0.36, 0.186 [45], 0.398 [46], 0.16 [47] |
| Diamond [44] | 1144.6 | 534.3 | 0.07 |
| D-AA+H | 794 | 375 | 0.06 |
| D-AB+H | 795 | 375 | 0.06 |
| D-AA | 1187 | 564 | 0.05 |
| D-AB | 1182 | 550 | 0.07 |
| H-diamane [14] | 692 | - | 0.08 |

with different lattice types. Since many properties can be dependent on the number of carbon layers, this work can be extended to analyze the stiffness and elastic constants of a multi-layered diamane.

*Acknowledgements. For M. R. T. and J. A. B. this research was funded by the State Assignement of IMSP RAS (Young scientist laboratory); for P. P. V., L. Kh. G. this research was funded by Grant of the Republic of Bashkortostan for young scientists; Calculation of the engineering elastic constants done by D. S. L. was supported by the Government program of IPMech RAS (Project 123021700045-7).*

## References

1. R. Dong, T. Zhang, X. Feng. Chem. Rev. 118 (13), 6189 (2018). Crossref
2. M. Xu, T. Liang, M. Shi, H. Chen. Chem. Rev. 113 (5), 3766 (2013). Crossref
3. A. K. Geim, K. S. Novoselov. Nat. Mater. 6 (3), 183 (2007). Crossref
4. G. Gupta, M. Zeng, A. Nurbawono, W. Huang, G. Liang. In: Graphene Science Handbook (ed. by M. Aliofkhazraei, N. Ali, W. I. Milne, S. Ozkan, S. Mitura, J. L. Gervasoni). Boca Raton, CRC Press (2016) pp. 209 – 226. Crossref
5. K. Nath, S. K. Ghosh, N. C. Das. In: Polymer Nanocomposites Containing Graphene (ed. by M. Rahaman, L. Nayak, I. A. Hussein, N. C. Das). Elsevier (2022) pp. 343 – 377. Crossref
6. S. Sagadevan, M. Z. Rahman, E. Lonard, D. Losic, V. Hessel. Nanomaterials. 13 (5), 846 (2023). Crossref
7. L. A. Chernozatonskii, P. B. Sorokin, A. G. Kvashnin, D. G. Kvashnin. JETP Letters. 90 (2), 134 (2009). Crossref
8. C. J. Wort, R. S. Balmer. Materials Today. 11 (1-2), 22 (2008). Crossref
9. A. R. Muniz, D. Maroudas. Phys. Rev. B. 86 (7), 075404 (2012). Crossref
10. S. Paul, K. Momeni. J. Phys. Chem. C. 123 (25), 15751 (2019). Crossref
11. Z. Zheng, H. Zhan, Y. Nie, X. Xu, D. Qi, Y. Gu. Carbon. 161, 809 (2020). Crossref
12. G. Qin, L. Wu, H. Gou. Function. Diam. 1 (1), 83 (2021). Crossref
13. P. V. Bakharev, M. Huang, M. Saxena, S. W. Lee, S. H. Joo, S. O. Park, J. Dong, D. C. Camacho-Mojica, S. Jin, Y. Kwon, M. Biswal, F. Ding, S. K. Kwak, Z. Lee, R. S. Ruoff. Nat. Nanotechnol. 15 (1), 59 (2019). Crossref
14. B. Mortazavi, F. Shojaei, B. Javvaji, M. Azizi, H. Zhan, T. Rabczuk, X. Zhuang. Appl. Surf. Sci. 528, 147035 (2020). Crossref
15. F. Piazza, M. Monthioux, P. Puech, I. C. Gerber, K. Gough. MDPI C — J. Carbon Research. 7 (1), 9 (2021). Crossref
16. F. Piazza, K. Cruz, M. Monthioux, P. Puech, I. Gerber. Carbon. 169, 129 (2020). Crossref
17. L. A. Chernozatonskii, P. B. Sorokin, A. A. Kuzubov, B. P. Sorokin, A. G. Kvashnin, D. G. Kvashnin, P. V. Avramov, B. I. Yakobson. J. Phys. Chem. C. 115 (1), 132 (2010). Crossref
18. L. A. Chernozatonskii, B. N. Mavrin, P. B. Sorokin. Phys. Status Solidi B. 249 (8), 1550 (2012). Crossref
19. R. S. Ruoff. MRS Bull. 37 (12), 1314 (2012). Crossref
20. G. Kresse, J. Furthmüller. Phys. Rev. B. 54 (16), 11169 (1996). Crossref
21. L. Zhu, W. Li, F. Ding. Nanoscale. 11 (10), 4248 (2019). Crossref
22. M. Raeisi, B. Mortazavi, E. V. Podryabinkin, F. Shojaei, X. Zhuang, A. V. Shapeev. Carbon. 167, 51 (2020). Crossref
23. V. A. Arsentiev, I. I. Blekhman, L. I. Blekhman, L. A. Weisberg, K. S. Ivanov, A. M. Krivtsov. Enrichment of Ruds. 1, 30 (2010).
24. I. E. Berinskii, A. M. Krivtsov. Mech. Solids. 45 (6), 815 (2010). Crossref
25. A. M. Krivtsov, E. A. Podol'skaya. Mech. Solids. 45 (3), 370 (2010). Crossref
26. Y.-C. Wu, J.-L. Shao, Z. Zheng, H. Zhan. J. Phys. Chem. C. 125 (1), 915 (2020). Crossref
27. A. R. Muniz, A. S. Machado, D. Maroudas. Carbon. 81, 663 (2015). Crossref
28. T. V. Vu, H. V. Phuc, S. Ahmad, V. Q. Nha, C. V. Lanh, D. P. Rai, A. I. Kartamyshev, K. D. Pham, L. C. Nhan, N. N. Hieu. RSC Advances. 11 (38), 23280 (2021). Crossref
29. LAMMPS Molecular Dynamics Simulator: Website
30. S. Plimpton. J. Comput. Phys. 117 (1), 1 (1995). Crossref
31. A. P. Thompson, H. M. Aktulga, R. Berger, D. S. Bolintineanu, W. M. Brown, P. S. Crozier, P. J. in 't Veld, A. Kohlmeyer, S. G. Moore, T. D. Nguyen, R. Shan, M. J. Stevens, J. Tranchida, C. Trott, S. J. Plimpton. Comput. Phys. Commun. 271, 108717 (2022). Crossref
32. S. J. Stuart, A. B. Tutein, J. A. Harrison. J. Chem. Phys. 112 (14), 6472 (2000). Crossref
33. M. A. Rozhkov, N. D. Abramenko, A. L. Kolesnikova, A. E. Romanov. Letter. Mater. 10 (4s), 551 (2020). Crossref
34. M. Garg, S. Ghosh, V. Padmanabhan. Letter. Mater. 11 (3), 321 (2021). Crossref
35. K. A. Bukreeva, A. M. Iskandarov, S. V. Dmitriev, Y. Umeno. Letter. Mater. 3 (4), 318 (2013). (in Russian) Crossref
36. R. I. Babicheva, S. V. Dmitriev, E. A. Korznikova, K. Zhou. J. Exp. Theor. Phys. 129 (1), 66 (2019). Crossref
37. M. Chen, A. R. Muniz, D. Maroudas. ACS Appl. Mater. Interfaces. 10 (34), 28898 (2018). Crossref
38. F. Mouhat, F.-X. Coudert. Phys. Revi. B. 90 (22), 224104 (2014). Crossref
39. A. Sakhaee-Pour. Solid State Commun. 149 (1-2), 91 (2009). Crossref
40. T. Pakornchote, A. Ektarawong, B. Alling, U. Pinsook, S. Tancharakorn, W. Busayaporn, T. Bovornratanaraks. Carbon. 146, 468 (2019). Crossref
41. M. Tahani, S. Safarian. J. Braz. Soc. Mech. Sci. Eng. 41 (1), 3 (2018). Crossref
42. H. J. McSkimin, P. Andreatch. J. Appl. Phys. 43 (7), 2944 (1972). Crossref
43. F. Cellini, F. Lavini, T. Cao, W. de Heer, C. Berger, A. Bongiorno, E. Riedo. FlatChem. 10, 8 (2018). Crossref
44. R. Pastorelli, A. Ferrari, M. Beghi, C. Bottani, J. Robertson. Diam. Relat. Mater. 9 (3-6), 825 (2000). Crossref

45. F. Liu, P. Ming, J. Li. Phys. Rev. B. 76 (6), 064120 (2007). Crossref
46. Q. Lu, R. Huang. Int. J. Appl. Mech. 01 (03), 443 (2009). Crossref
47. T. Chang, H. Gao. J. Mech. Phys. Solids. 51 (6), 1059 (2003). Crossref
48. K. V. Zakharchenko, M. I. Katsnelson, A. Fasolino. Phys. Rev. Lett. 102 (4), 046808 (2009). Crossref
49. G. Kalosakas, N. N. Lathiotakis, C. Galiotis, K. Papagelis. J. Appl. Phys. 113 (13), 134307 (2013). Crossref
50. E. Barborini, P. Piseri, P. Milani, G. Benedek, C. Ducati, J. Robertson. Appl. Phys. Lett. 81 (18), 3359 (2002). Crossref
51. S.-J. Cho, K.-R. Lee, K. Y. Eun, J. H. Hahn, D.-H. Ko. Thin Solid Films. 341 (1-2), 207 (1999). Crossref
52. N. Savvides, T. J. Bell. J. Appl. Phys. 72 (7), 2791 (1992). Crossref
53. A. G. Kvashnin, P. B. Sorokin. J. Phys. Chem. 5 (3), 541 (2014). Crossref